




## RESEARCH ARTICLE

## Exploring the effect of dynamic bond placement in liquid crystal elastomers

Charlie A. Lindberg<sup>1</sup>  | Elina Ghimire<sup>1</sup> | Chuqiao Chen<sup>1</sup> | Sean Lee<sup>2</sup> |  
 Neil D. Dolinski<sup>1</sup>  | Joseph M. Dennis<sup>3</sup> | Sihong Wang<sup>1</sup> | Juan J. de Pablo<sup>1,4</sup> |  
 Stuart J. Rowan<sup>1,2,4</sup> 

<sup>1</sup>Pritzker School of Molecular Engineering, University of Chicago, Chicago, Illinois, USA

<sup>2</sup>Department of Chemistry, University of Chicago, Chicago, Illinois, USA

<sup>3</sup>Sciences of Extreme Materials Division, Polymers Branch, U.S. DEVCOM Army Research Laboratory, Aberdeen, Maryland, USA

<sup>4</sup>Center for Molecular Engineering, Argonne National Lab, Lemont, Illinois, USA

## Correspondence

Stuart J. Rowan, Pritzker School of Molecular Engineering, University of Chicago, 5640 S. Ellis Ave., Chicago, IL 60637, USA.

Email: [stuartrowan@uchicago.edu](mailto:stuartrowan@uchicago.edu)

## Funding information

Army Research Laboratory, Grant/Award Number: W911NF-20-2-0044; National Science Foundation, Grant/Award Numbers: 2011854, 1844463

## Abstract

Dynamic liquid crystal elastomers (LCEs) are a class of polymer networks characterized by the inclusion of both liquid crystalline monomers and dynamic covalent bonds. The unique properties realized through the combination of these moieties has produced a plethora of stimuli-responsive materials to address a range of emerging technologies. While previous works have studied the incorporation of different dynamic bonds in LCEs, few (if any) have studied the effect of the specific placement of the dynamic bonds within an LCE network. A series of dynamic LCE networks were synthesized using a generalizable approach that employs a tandem thiol-ene/yne chemistry which allows the location of the dynamic disulfide bond to be varied while maintaining similar network characteristics. When probing these systems in the LC regime, the thermomechanical properties were found to be largely similar. It is not until elevated temperatures (160–180 °C) that differences in the relaxation activation energies of these systems begin to materialize based solely on differences in placement of the dynamic bond throughout the network. This work demonstrates that through intentional dynamic bond placement, stress relaxation times can be tuned without affecting the LCE character. This insight can help optimize future dynamic LCE designs and achieve shorter processing times.

## KEYWORDS

click chemistry, disulfides, dynamic chemistry, liquid crystal elastomers, networks

## 1 | INTRODUCTION

Liquid crystal elastomers (LCEs) are a class of soft materials characterized by the incorporation of mesogenic monomers into a crosslinked polymer network.<sup>1,2</sup>

Generally, the tethered mesogens form randomly-oriented but locally-aligned domains in what is referred to as a polydomain LCE. If the film is prepared in a manner that all the mesogens are aligned in the same direction, then the result is a “monodomain” LCE. Traversing

This is an open access article under the terms of the [Creative Commons Attribution-NonCommercial-NoDerivs](https://creativecommons.org/licenses/by-nc-nd/4.0/) License, which permits use and distribution in any medium, provided the original work is properly cited, the use is non-commercial and no modifications or adaptations are made.

© 2023 The Authors. *Journal of Polymer Science* published by Wiley Periodicals LLC.

the LC to isotropic transition, via stimuli such as heat,<sup>3</sup> light,<sup>4</sup> humidity,<sup>5</sup> or metal ions,<sup>6</sup> can result in responsive properties such as shape memory and optical responsiveness. Another key feature of these materials is their “soft elasticity” which refers to their ability to dissipate stress through mesogenic rotational modes when an LCE is sufficiently stressed to strains outside of its specific linear viscoelastic regime.<sup>7</sup> Given these unique properties, LCEs have received much attention for emerging applications in soft robotics,<sup>8,9</sup> medical devices,<sup>10,11</sup> and adaptive optics.<sup>12,13</sup>

Traditionally, monodomain LCEs are accessed via either the alignment of the LC monomers prior to crosslinking or the utilization of a two-step crosslinking approach where materials are partially crosslinked, mechanically strained, and then fully crosslinked to lock in the aligned state as the permanent mesogenic configuration.<sup>3,14–16</sup> However, as these processes typically involve inducing alignment of viscous solutions or handling and manipulating fragile, still reactive materials, the scale and physical form that these LCEs can take is limited. Additionally, as is expected for a permanently crosslinked network, once the crosslinking reaction has been completed these materials are fixed with the alignment and shape they were crosslinked with and can no longer be reset or reprocessed.

A more recent development in LCEs has been the introduction of dynamic covalent chemistries into the structure of the network.<sup>17–19</sup> A dynamic covalent bond has the ability to be broken and reformed, ideally without any irreversible side reactions.<sup>20,21</sup> In addition to facilitating bulk reprocessability and enhancing stress relaxation/dissipation in LCEs, the dynamic bonds also provide a route to (re)program the LCEs after they have been crosslinked. By manipulating the mesogen alignment while simultaneously activating the dynamic bond, it is possible to utilize the dynamic exchange processes to promote network reorganization such that stable alignment is post-synthetically programmed upon bond reformation. A wide range of dynamic chemistries have been utilized in LCEs over the past decade including transesterification,<sup>22–24</sup> disulfide exchange,<sup>25–27</sup> and addition fragmentation transfer reactions<sup>28–31</sup> to name a few.

Of these dynamic bonds, disulfides stand out as a particularly useful dynamic chemistry for a multitude of reasons. The disulfide (Figure 1A), with a bond energy of around 60 kcal mol<sup>−1</sup> (251 kJ mol<sup>−1</sup>), is a well-studied multi-responsive dynamic bond, capable of being activated using a host of stimuli including heat,<sup>32,33</sup> UV light,<sup>34,35</sup> redox,<sup>36</sup> shear,<sup>37</sup> ultrasound,<sup>38</sup> and chemical catalysts.<sup>39</sup> The formed thiyl radicals (or thiolate ions) are also capable of exchanging with existing disulfide bonds through an associative process (Figure 1A) that occurs at a much faster rate than exchange mediated by the

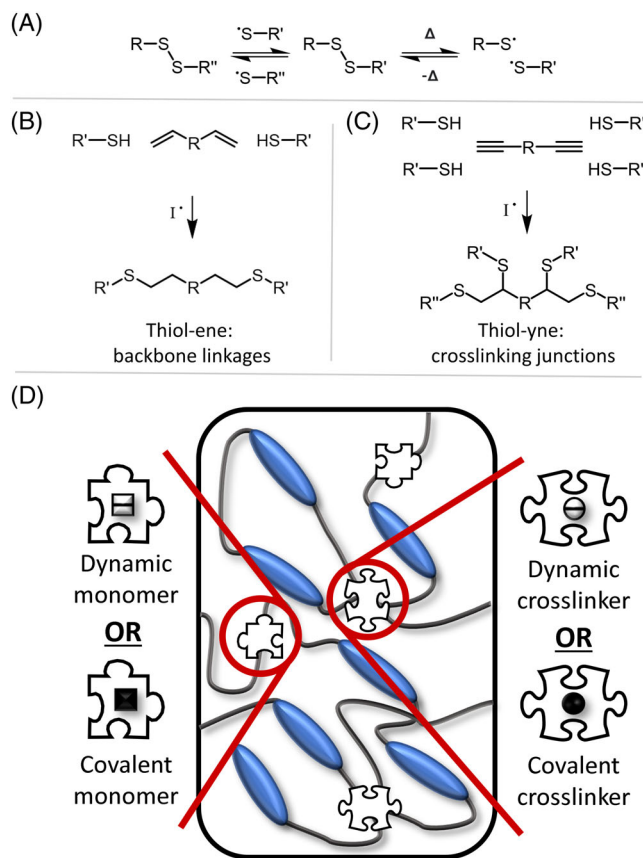


**FIGURE 1** (A). Dynamic exchange of disulfide bonds; (B). Radical initiated reaction mechanism for a dialkene monomer with two thiols forming a linear backbone linkage; (C). Radical initiated reaction mechanism for a dialkyne crosslinker with four thiols forming a crosslink; (D). Schematic depicting the modular nature of this dynamic LCE system that allows for selective disulfide placement in backbone linkages, crosslinks, or both.

sequential breaking and reforming of disulfides.<sup>40</sup> Naturally, disulfides have been extended to LCEs, with a number of works incorporating disulfides into materials to achieve enhanced reprocessability and post-synthetic alignment capabilities.<sup>13,25–27,41–44</sup> However, among these reports, the routes for installing disulfides into LCEs vary greatly and include crosslinking through oxidizing thiols to disulfides,<sup>25,27,42,43</sup> incorporating monomers with pre-formed disulfide linkages,<sup>26,41</sup> or ring opening cyclic disulfides to form LCEs with polydisulfide backbones.<sup>44</sup> It is worth noting that in these dynamic LCEs the location of the disulfide bond within the network is never expressly considered, and the disulfide is free to exist in the network anywhere the components or the chemistries permit. This ultimately produces systems where the disulfide placement is either random or hyper regular making it impossible to directly compare these systems from the perspective of dynamic LCE design. As topology is a critical factor when considering any polymer network,

it stands to reason that dynamic topology, specifically the placement of the dynamic bond throughout the network, is also of critical importance when it comes to considering dynamic network materials and their properties. However, to properly test the impact of dynamic bond placement, the overall network characteristics must be held constant to isolate the impact of dynamic bond location.

A benefit of exploring the impact of dynamic bond location in LCEs comes from the ability to track programmed mesogen alignment, which directly correlates to the efficacy of network reorganization resulting from dynamic bond exchange. As such, the goal of this work was to design and synthesize a series of modular disulfide-containing LCEs to elucidate the effect that the topological placement of dynamic bonds plays on linear and nonlinear thermomechanical properties across different timescales. More specifically the use of a tandem thiol-ene/yne approach was explored to allow for locking in key network characteristics (glass transition temperature ( $T_g$ ), nematic to isotropic transition temperature ( $T_{NI}$ ), plateau modulus, etc.) while systematically varying the location of the dynamic moieties.

As click chemistries, thiol-ene and thiol-yne reactions have been well-studied in polymers, in large part for their rapid initiation and high efficiencies.<sup>45–47</sup> Given that both alkene and alkyne bonds are capable of reacting with thiols through a radically initiated pathway where one alkene can react with one thiol and one alkyne can react with two thiols, it follows that provided with a stoichiometric amount of thiol, both alkene and alkyne moieties can be incorporated into a single network using the same initiation process. As such, the current system consists of dialkene species that serve as linear components (Figure 1B) and dialkyne species that serve as crosslinkers (Figure 1C). Based on this concept, networks synthesized from a series of dynamic and covalent components based on thiol-alkene/alkyne chemistry would allow for the controlled placement of a dynamic bond within an otherwise identical LCE framework (Figure 1D). For this work, a modular dynamic LCE system was devised using the disulfide bond as a multiresponsive dynamic linkage (Figure 1A), installed via a tandem thiol-ene/yne chemistry to allow for differentiation in bond placement based solely on component functionality.

## 2 | RESULTS AND DISCUSSION

To best isolate the effect of dynamic bond location as a variable within a dynamic LCE material, a series of design criteria were followed that include (1) utilizing molecularly similar monomers to minimize differences in

intermolecular interactions between non-LC components; (2) thermally separating the LC transition temperature from the temperature where most disulfide bonds have been cleaved ( $>150^\circ\text{C}$ )<sup>33</sup>; and (3) targeting a constant concentration of disulfide bonds within the network across the materials studied. The first criterion serves to minimize differences in the structure and properties of the networks outside of the placement of the dynamic bonds. The second criterion ensures that there is sufficient thermal isolation of the disulfide from the liquid crystalline transition so the similarity in LCE properties can be verified without convolution of relaxation events that occur on account of significant dynamic bond exchange. The final criterion ensures that the concentration of disulfide bonds present in any dynamic network studied is constant, so observed variations are decoupled from differences in the amount of dynamic character. To satisfy the first criterion, a series of components including a LC monomer (**1**), a dynamic monomer (**2D**), a covalent monomer (**2C**), a dynamic crosslinker (**3D**), and a covalent crosslinker (**3C**) were synthesized based on previously reported literature procedures (see [Supporting Information](#) for complete synthetic details).<sup>48,49</sup> For the design of the non-LC components, a constant number of atoms along the molecule's primary axis was targeted while ester linkages were used to maintain similar polarity and secondary interactions. To satisfy the second criterion, the  $T_{NI}$  of the material system was tuned using the ratio of LC (**1**) to non-LC monomers (**2**) as it has been demonstrated previously in literature that the concentration of LC content in the feedstock can be used as a means of tuning the phase behavior for a given LCE.<sup>50</sup> A ratio of 3:1 was chosen for **1:2** as this ratio targets a material with a  $T_{NI}$  of around  $70^\circ\text{C}$  which falls between ambient conditions and where there is significant cleavage of the dynamic bond ( $>150^\circ\text{C}$ ) in order to limit the impact of thermally-induced disulfide cleavage on the LCEs' properties.

For the final criterion, it was necessary to find a ratio of components that allowed for the same amount of disulfide to be present in both the backbone as well as in the crosslinks. To achieve this, the molar ratio of non-LC alkene functionalized monomers (**2C** + **2D**) and alkyne functionalized crosslinkers (**3C** + **3D**) was set to be equivalent ensuring that the concentration of disulfide would be consistent across materials with different dynamic bond placements. Setting to this alkene/alkyne ratio should result in a molecular weight between crosslinks of ca.  $3000\text{ g mol}^{-1}$ .

Using the components and design criteria outlined above, a series of networks were synthesized where only the location of the disulfide itself is varied within the network. Three different dynamic LCEs with a constant

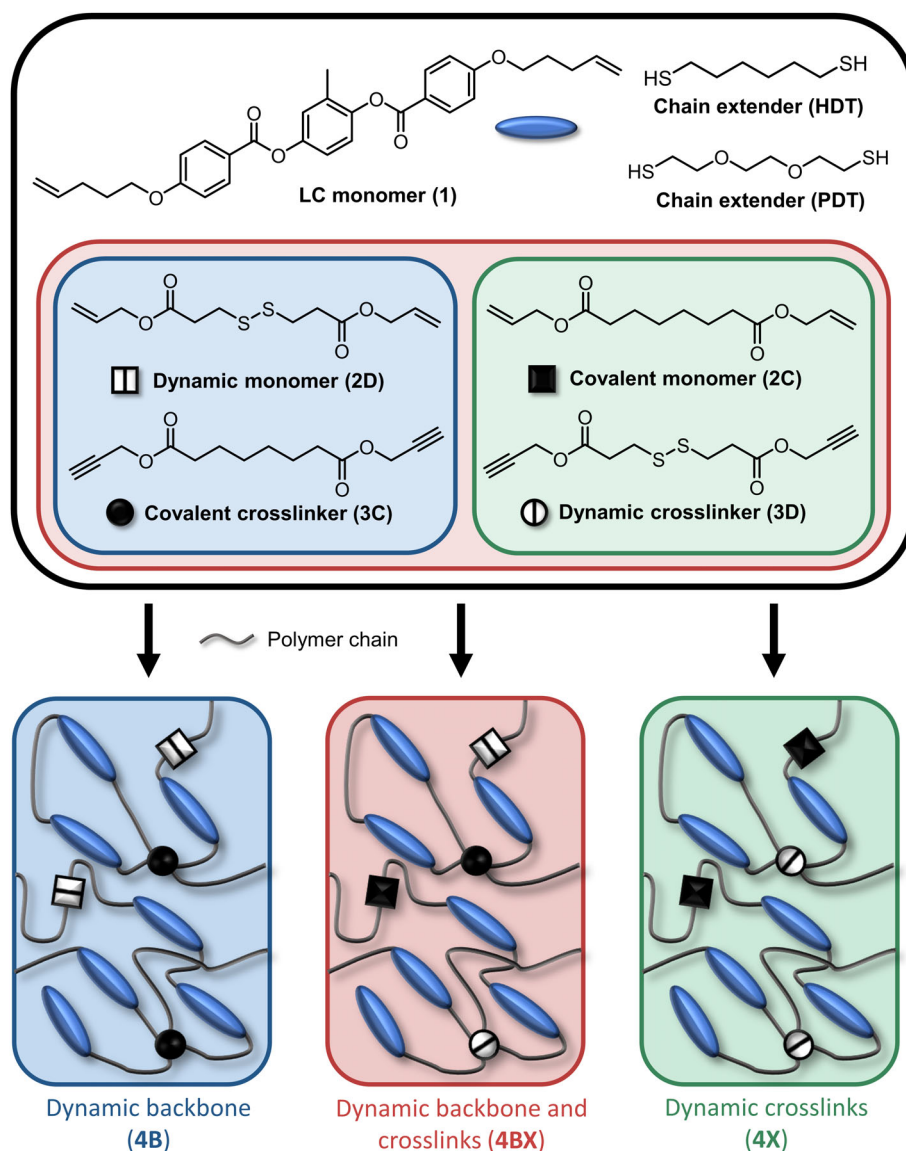


**FIGURE 2** Component and network designs for a modular disulfide containing LCE network that allows for selective disulfide placement in backbone linkages, crosslinks, and a system containing both.

concentration of disulfide were targeted (Figure 2): a network where the disulfide is located in 25% of the repeat units within the backbone (4B, formed using 2D and 3C), a network where the disulfide is located in every crosslink (4X, formed using 2C and 3D), and a network where the concentration of disulfide is split between both the backbone and crosslinks (4BX, formed using half molar equivalents of 2D, 2C, 3D, and 3C). A nondynamic control LCE (4N, formed using 2C and 3C) that contains no dynamic bonds was also synthesized to determine the impact that incorporating disulfide bonds into these LCE networks has on their bulk thermomechanical properties. A mixture of the dithiol chain extenders 1,6-hexanedithiol (HDT) and 2,2'-(ethylenedioxy)diethanethiol (PDT) was selected to inhibit crystallization.<sup>51,52</sup> To synthesize these materials, calculated quantities obtained through use of Carother's equation<sup>53</sup> of alkene functionalized monomers (1, 2C, 2D), dithiol chain extenders HDT and PDT, and alkyne

functionalized crosslinker (3C, 3D) were dissolved in tetrahydrofuran (THF) with a catalytic amount of the photoinitiator 2,2-dimethoxy-2-phenylacetophenone (DMPA). The reaction mixture was then cured through exposure to UV light (320–390 nm, 100 mW cm<sup>-2</sup>, 2 × 30 s) to yield a solid film. While potential UV-induced cleavage of the disulfide can result in thiyl species capable of reacting with alkenes and alkynes, previous works have shown the effect of these reactions to be minimal. For instance, Bongiardina et al. and Soars et al. both demonstrated a large difference in efficiency between reactions initiated by thiol generated radicals and those generated by cleaved disulfides for photo-mediated polymerizations.<sup>54,55</sup> Additionally, work by Kamps et al. demonstrated the low reactivity of aliphatic alkenes with photocleaved disulfides under ambient conditions in a study of the photodisulfidation of aliphatic alkenes.<sup>56</sup> To ensure the removal of any unreacted monomers from the



dynamic LCEs, the films were then cut into pieces and washed with THF and methanol (MeOH) using a Soxhlet extractor. After drying under vacuum (16 h, 60 °C), the materials were melt processed under pressure (1 h, 180 °C, 4 tons) to homogenize the materials into films. Gel fractions were taken for the materials and ranged from 87 to 89 wt%. Thermogravimetric analysis was also performed to confirm the removal of solvent and unreacted starting materials (Figure S1).

To assess the thermal transitions of the prepared LCEs, differential scanning calorimetry (DSC) was employed (Figure 3A). Analysis of the DSC thermograms reveals only a minor effect in incorporating disulfide bonds into LCEs when comparing the non-dynamic **4N** to the disulfide-containing **4B**, **4BX**, and **4X** that manifests as a 3–6 °C decrease in both the glass  $T_g$  and  $T_{NI}$ . However, the  $T_g$ s and  $T_{NI}$ s as measured in DSC, ca. –33 °C and 71 °C respectively, for the dynamic LCEs **4B**, **4BX**, and **4X** fall within a few degrees of one another. This suggests that placement of the disulfide bond does not have a large impact on the liquid crystalline

transition, implying that the bond placement does not strongly impact the packing stability of the mesogenic units. The similarity in thermal properties was corroborated by the small angle oscillatory shear (SAOS) rheology data (Figure 3B). The measured storage modulus ( $G'$ ) for all samples were found to nearly overlap across the entire temperature range probed (–50 °C to 180 °C). A steep decrease in the  $G'$  curve as well as a peak in the  $\tan(\delta)$  curve corresponding to the  $T_g$  appears ca. –17 °C for all materials which further confirms that a consistent set of thermal properties was achieved. A shoulder from 10 °C to 70 °C in the  $\tan(\delta)$  curve is indicative of the nematic character of the networks and has been reported for previously studied LCEs.<sup>57</sup> Around 70 °C, a minimum in the  $G'$  curve and a corresponding step in the  $\tan(\delta)$  curve (commonly ascribed to the  $T_{NI}$  for an LCE<sup>57</sup>) further demonstrate congruence in the liquid crystalline character of the dynamic materials and is in line with the trend observed in the DSC data. These data serve to establish the similarity of these materials despite their varied dynamic bond placement. To probe the nonlinear properties of the dynamic LCEs, tensile tests, dynamically programmed alignment, and wide-angle x-ray scattering (WAXS) experiments were performed on the series of dynamic materials to determine if dynamic bond placement alters the structural arrangement of the network in the nonlinear/high strain regime where LC alignment is induced.

To determine the programming strain conditions, tensile tests were performed under ambient conditions (22 °C) on rectangular samples of **4B**, **4BX**, and **4X**, where the materials were elongated at a constant rate (5 mm min<sup>–1</sup>) until failure. Much in line with the trends observed thus far, all measured tensile curves appear highly similar (Figure S2), suggesting that nonlinear tensile behavior under ambient conditions does not appear to be impacted by the placement of the disulfide bond within the network. A representative tensile curve of **4B** (Figure 4A) demonstrates the different mechanical regimes inherent to LCEs.<sup>2</sup> At low strains (0%–10% strain), the material possesses a primarily elastic response dominated by the LC domains. At intermediate strains (10%–60% strain) the material passes into a soft elastic state characterized by a plateau with a low change in stress, as stress is primarily being dissipated by mesogens rotating throughout the material. Once the majority of the mesogens are rotated such that their alignment is in the direction of the stress, the material enters a strain hardening regime (60%–150% strain) where the slope of the tensile curve begins to increase as the network increasingly resists alignment.

Utilizing the stress–strain profiles, a rectangular sample of each material was subjected to a programming process adapted from literature<sup>25</sup> to determine how dynamic network reorganization in the aligned nematic phase is affected by the location of the disulfide bond. In order to

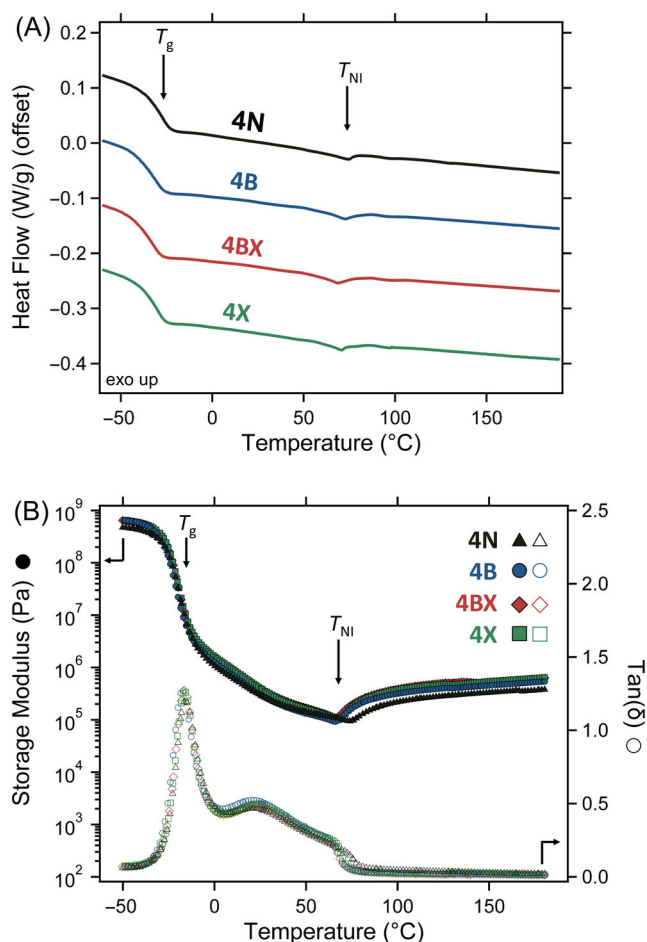


**FIGURE 3** (A). Differential scanning calorimetry thermograms of dynamic liquid crystal elastomer films; (B). Shear rheology dynamic temperature ramps of storage modulus (solid shapes) and  $\tan(\delta)$  (empty shapes) for dynamic LCEs.

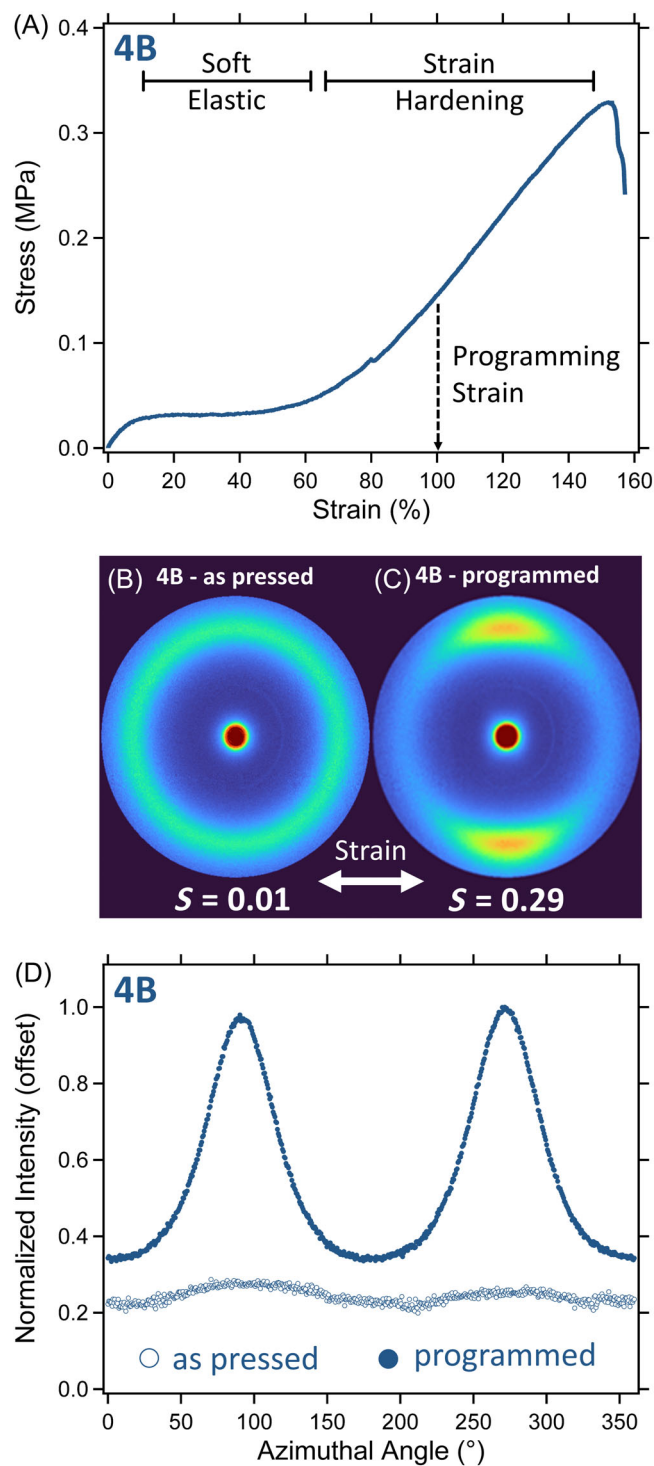


**FIGURE 4** (A). Stress–strain profile of an as pressed sample of **4B**; (B). 2D WAXS image of an as pressed film of **4B**; (C). 2D WAXS image of an aligned programmed film of **4B**; (D). Plots of normalized intensity as a function of angle for both an as pressed and programmed aligned film of **4B**.

remain below  $T_{NI}$  and preserve mesogen alignment, UV light was used as a dynamic stimulus to trigger disulfide exchange.<sup>25,42</sup> For this process, the samples were stretched to 100% strain in the strain-hardening regime

(to ensure rotation of the majority of mesogens had been induced). The samples were then fixed at this strain between two glass slides and then exposed to UV light (320–390 nm, 200 mW cm<sup>−2</sup>) for 15 min on each side. Upon removing the samples from the slides, they were heated above their  $T_{NI}$  to induce a contraction to their initial state, and upon cooling, the materials adopted their new dynamically programmed elongated state.

To quantify the extent of alignment, WAXS measurements were taken on as pressed **4B**, **4BX**, and **4X** as well as their dynamically programmed counterparts. The as pressed **4B** displays an isotropic 2D WAXS pattern (Figure 4B) indicative of the statistical alignment of the domains in the polydomain material at every angle demonstrating the lack of overall alignment in the sample. For the dynamically aligned sample of **4B** (Figure 4C) the 2D pattern clearly changes to that of an anisotropic response with increased intensity of scattering in the vertical axis which indicates preferential alignment of the mesogens in the horizontal axis along which strain has been applied. Upon analyzing the plot of intensity as a function of azimuthal angle (Figure 4D), it becomes apparent that a significant change in alignment character has been imposed on the dynamically aligned sample. The fitting of these plots using the Kratky method<sup>58</sup> allows for the calculation of the Hermans order parameter ( $S$ )<sup>59</sup> for these systems where the as pressed material has an order parameter of  $S = 0.01$  while dynamically programmed sample has an order parameter of  $S = 0.29$ . Critically, this trend holds true for the other materials as well with **4BX** (Figure S3) having order parameters of  $S = 0.01$  and  $S = 0.29$  for the as pressed and dynamically programmed respectively and **4X** (Figure S4) having order parameters of  $S = 0.03$  and  $S = 0.30$  for the as pressed and dynamically programmed respectively. This similarity in values not only suggests that the reorganization process under strain conditions can be achieved utilizing the multi-responsive character of the disulfide bond, but also that under this set of ambient and active nonlinear conditions important for LCE actuation, the placement of the disulfide does not hinder the processes required for network reorganization. Up to this point, it has been demonstrated that the placement of the disulfide within the LCE network has seemingly not impacted the materials' properties. However, it is important to note that so far, the testing was done either in the nematic state where LC interactions are engaged or using methods that probe short relaxation time-scales (at sufficiently low temperatures) within the material.

To isolate the impact of the location of the disulfide bonds, high temperature (i.e., well above the  $T_{NI}$  of ca. 70 °C) shear stress relaxation studies were performed on the dynamic LCEs. Figure 5 shows the stress relaxation behavior in the linear viscoelastic regime (Figure S5) for **4B**, **4BX**, and **4X** across a range of temperatures from

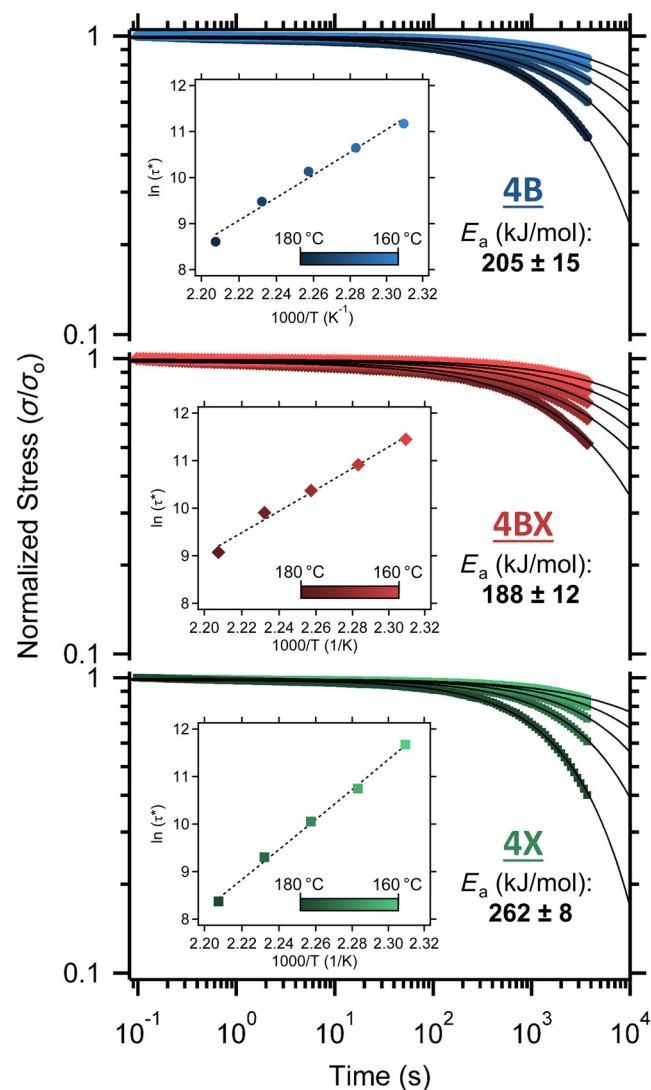


**FIGURE 5** Temperature dependent stress relaxation curves for dynamic LCEs fitted to stretched exponential functions, with  $\tau^*$  values determined by the fit. (Inset) Arrhenius curves demonstrating the linear relationship between  $\ln(\tau^*)$  and temperature for a given sample. Errors for activation energies are derived from the linear fit of the data.

160 °C to 180 °C (3% strain, 1 h), which represent an experimentally active window (that maintains Arrhenius behavior<sup>60,61</sup>) for the disulfide exchange. A stretched exponential relaxation model was used to fit the data (fit parameters shown in Figure S6), which allowed for acquisition of characteristic relaxation times ( $\tau^*$ ) for these highly viscous systems where the characteristic relaxation time is defined as the time needed for the initial stress to decay to  $1/e$  of its initial value. As shown in the insets for Figure 5, the fitted  $\tau^*$  values across the measured range behave in an Arrhenius fashion. Interestingly, the activation energy of relaxation for **4B** and **4X** were found to be starkly different. The **4B** sample was found to have a considerably smaller activation energy of relaxation relative to **4X** ( $205 \pm 15$  vs.  $262 \pm 8$  kJ mol<sup>-1</sup>).

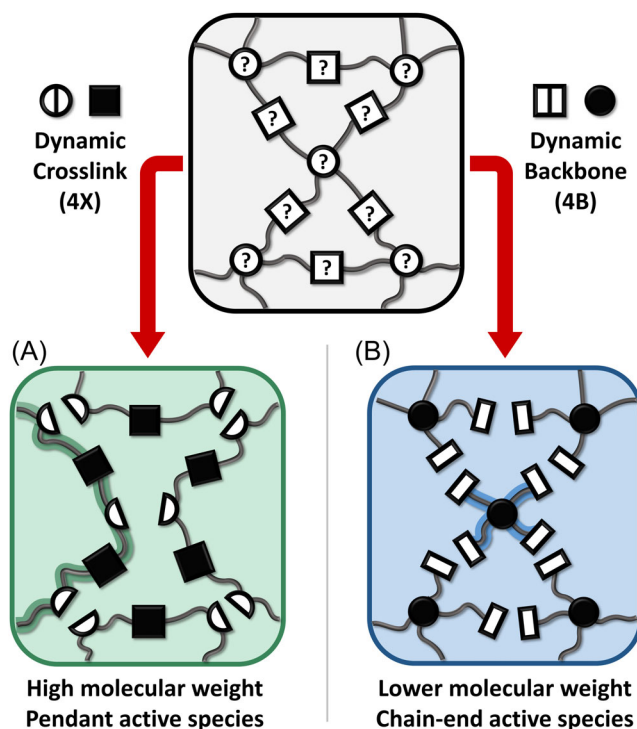


**FIGURE 6** (A) A schematic of the higher molecular weight, lower relative mobility pendant active species formed by the cleavage of a disulfide in a material with only dynamic crosslinks (**4X**); (B) A schematic of the lower molecular weight, higher relative mobility chain-end active species formed by the cleavage of a disulfide in a material with only a dynamic backbone (**4B**).

For reference the reported values of the activation energy of a disulfide bond is ca. 251 kJ mol<sup>-1</sup>.<sup>62</sup> The activation energy of relaxation of **4BX** ( $188 \pm 12$  kJ mol<sup>-1</sup>) was found to be within error of **4B** film, suggesting that the backbone-based relaxation processes dominate this film's overall relaxation behavior.

It is hypothesized that the observed differences in activation energies between systems with differing dynamic bond location stem from the ability of the disulfide to effectively exchange under these conditions. As demonstrated in recent work by Lessard et al., diffusion of species has been shown to play an important role in the relaxation processes of dynamic covalent networks, where increases in molecular weight (and therefore lower diffusability) resulted in higher activation flow energies, slower relaxations, and lower recovery flow rates.<sup>63</sup> From a dynamic topology perspective, significant disulfide cleavage in the case of a material that is only dynamic at the crosslinks would result in very high molecular weight linear polymer species. The diffusion of this type of high molecular weight species and its ability to exchange are limited by the movement of the entire polymer chain resulting in lower mobility towards finding an exchange partner (Figure 6A). However, in the



idealized case of significant disulfide bond cleavage in a material with backbone-placed disulfides, an unbound lower molecular weight species ( $\sim 6 \text{ kg mol}^{-1}$  4-arm stars) should theoretically be formed free from the network where the active thiyl radicals exist at the free species' chain-ends (Figure 6B). This decrease in the molecular weight associated with the free species would suggest a greater diffusability for the active thiyl radicals and a greater chance of finding a disulfide to exchange with. Therefore, it is possible to tune the activation energy for the relaxation processes in a dynamic LCE by controlling the architecture of the active species formed under conditions where the dynamic bond is active.

### 3 | CONCLUSION

In this work, a tandem thiol-ene/yne strategy for synthesizing disulfide-containing LCEs was developed where the topological location of the dynamic bond was modified through targeted choice of network components with different functional handles. Characteristic thermal transitions such as the  $T_g$  and  $T_{NI}$  were found to be consistent between DSC and SAOS rheology. Additionally, the post-synthetic programming capability of these dynamic materials was found to be consistent between the different placements of the dynamic bond with the achieved order parameter being similar for the suite of dynamic materials. However, at higher temperatures, temperature-dependent stress relaxation experiments demonstrated a divergence in properties where materials with disulfides only located in crosslinks (4X) have a markedly higher activation energy than materials that incorporate disulfides into backbone linkages (4B and 4BX). These results suggest that designing dynamic species with high degrees of diffusability for the active species can result in lower activation energies for relaxation processes, and future works can adopt these design principles as a means of altering properties like processing time without changing other material properties or the chemistry being utilized. As such this provides an additional method of tuning the programmability of dynamic LCEs and the overall processing of other types of dynamic networks.

### 4 | EXPERIMENTAL MATERIALS AND METHODS

See [Supporting Information](#) for full experimental details.

#### ACKNOWLEDGMENTS

Parts of this work were carried out at the Soft Matter Characterization Facility and the Materials

Research Science and Engineering Center (MRSEC NSF DMR-2011854) at the University of Chicago. The views and conclusions contained in this document are those of the authors and should not be interpreted as representing the official policies, either expressed or implied, of the Army Research Laboratory, or the U.S. Government. The U.S. Government is authorized to reproduce and distribute reprints for Government purposes notwithstanding any copyright notation herein.

#### FUNDING INFORMATION

This work was primarily supported by the University of Chicago Materials Research Science and Engineering Center (IRG1) which is funded by the National Science Foundation under award number DMR-2011854. Chuqiao Chen was supported by a University of Chicago MRSEC Fellowship. Sean Lee was supported by a Partnership in International Research and Education Grant by the National Science Foundation Grant, DMR-1844463. Joseph M. Dennis was sponsored by the Army Research Laboratory under Cooperative Agreement Number W911NF-20-2-0044.

#### CONFLICT OF INTEREST STATEMENT

The authors declare they have no conflicts of interest.

#### DATA AVAILABILITY STATEMENT

The data that support the findings of this study are available from the corresponding author upon reasonable request.

#### ORCID

Charlie A. Lindberg  <https://orcid.org/0000-0001-8391-4753>

Neil D. Dolinski  <https://orcid.org/0000-0002-2160-8811>

Stuart J. Rowan  <https://orcid.org/0000-0001-8176-0594>

#### REFERENCES

- [1] P. G. De Gennes, *C R Acad. Sci. B* **1975**, 281, 101.
- [2] M. Warner, E. M. Terentjev, *International Series of Monographs on Physics: Liquid Crystal Elastomers*, Oxford University Press, Oxford **2007**.
- [3] J. Kupfer, H. Finkelmann, *Makromol. Chem. Rapid Commun.* **1991**, 12, 717.
- [4] T. Ube, K. Kawasaki, T. Ikeda, *Adv. Mater.* **2016**, 28, 8212.
- [5] L. T. De Haan, J. M. N. Verjans, D. J. Broer, C. W. M. Bastiaansen, A. P. H. J. Schenning, *J. Am. Chem. Soc.* **2014**, 136, 10585.
- [6] B. T. Michal, B. M. McKenzie, S. E. Felder, S. J. Rowan, *Macromolecules* **2015**, 48, 3239.
- [7] M. Warner, P. Bladon, E. M. Terentjev, *J. Phys. II* **1994**, 4, 93.
- [8] A. Kotikian, C. McMahan, E. C. Davidson, J. M. Muhammad, R. D. Weeks, C. Daraio, J. A. Lewis, *Sci. Robot.* **2019**, 4, eaax7044.
- [9] Q. He, Z. Wang, Y. Wang, A. Minori, M. T. Tolley, S. Cai, *Sci. Adv.* **2019**, 5, eaax574.
- [10] R. H. Volpe, D. Mistry, V. V. Patel, R. R. Patel, C. M. Yakacki, *Adv. Healthc. Mater.* **2020**, 9, 1901136.



- [11] N. A. Traugutt, D. Mistry, C. Luo, K. Yu, Q. Ge, C. M. Yakacki, *Adv. Mater.* **2020**, 32, 2000797.
- [12] M. T. Brannum, A. M. Steele, M. C. Venetos, L. T. J. Korley, G. E. Wnek, T. J. White, *Adv. Opt. Mater.* **2019**, 7, 1801683.
- [13] S. Hussain, S. Y. Park, *ACS Appl. Mater. Interfaces* **2021**, 13, 59275.
- [14] T. H. Ware, Z. P. Perry, C. M. Middleton, S. T. Iacono, T. J. White, *ACS Macro Lett.* **2015**, 4, 942.
- [15] T. Guin, B. A. Kowalski, R. Rao, A. D. Auguste, C. A. Grabowski, P. F. Lloyd, V. P. Tondiglia, B. Maruyama, R. A. Vaia, T. J. White, *ACS Appl. Mater. Interfaces* **2018**, 10, 1187. <https://doi.org/10.1021/acsami.7b13814>
- [16] C. M. Yakacki, M. Saed, D. P. Nair, T. Gong, S. M. Reed, C. N. Bowman, *RSC Adv.* **2015**, 5, 18997.
- [17] Z. Wang, S. Cai, *J. Mater. Chem. B* **2020**, 8, 6610.
- [18] M. O. Saed, A. Gablier, E. M. Terentjev, *Chem. Rev.* **2022**, 122, 4927.
- [19] C. Valenzuela, Y. Chen, L. Wang, W. Feng, *Chemistry* **2022**, 28, e202201957.
- [20] S. J. Rowan, S. J. Cantrill, G. R. L. Cousins, J. K. M. Sanders, J. F. Stoddart, *Angew. Chem. Int. Ed.* **2002**, 41, 898.
- [21] R. J. Wojtecki, M. A. Meador, S. J. Rowan, *Nat. Mater.* **2011**, 10, 14.
- [22] Z. Pei, Y. Yang, Q. Chen, E. M. Terentjev, Y. Wei, Y. Ji, *Nat. Mater.* **2014**, 13, 36.
- [23] H. Tsunoda, K. Kawasaki, T. Ube, T. Ikeda, *Mol. Cryst. Liq. Cryst.* **2018**, 662, 61.
- [24] D. W. Hanzon, N. A. Traugutt, M. K. McBride, C. N. Bowman, C. M. Yakacki, K. Yu, *Soft Matter* **2018**, 14, 951.
- [25] Z. Wang, H. Tian, Q. He, S. Cai, *ACS Appl. Mater. Interfaces* **2017**, 9, 33119.
- [26] L. Chen, M. Wang, L. X. Guo, B. P. Lin, H. Yang, *J. Mater. Chem. C* **2018**, 6, 8251.
- [27] D. Tang, L. Zhang, X. Zhang, L. Xu, K. Li, A. Zhang, *ACS Appl. Mater. Interfaces* **2022**, 14, 14.
- [28] M. K. McBride, M. Hendrikx, D. Liu, B. T. Worrell, D. J. Broer, C. N. Bowman, *Adv. Mater.* **2017**, 29, 1606509.
- [29] M. K. McBride, A. M. Martinez, L. Cox, M. Alim, K. Childress, M. Beiswinger, M. Podgorski, B. T. Worrell, J. Killgore, C. N. Bowman, *Sci. Adv.* **2018**, 4, eaat4634.
- [30] Z. S. Davidson, H. Shahsavan, A. Aghakhani, Y. Guo, L. Hines, Y. Xia, S. Yang, M. Sitti, *Sci. Adv.* **2019**, 5, eaay0855.
- [31] E. C. Davidson, A. Kotikian, S. Li, J. Aizenberg, J. A. Lewis, *Adv. Mater.* **2020**, 32, 1905682.
- [32] L. Zhang, S. J. Rowan, *Macromolecules* **2017**, 50, 5051.
- [33] L. Imbernon, E. K. Oikonomou, S. Norvez, L. Leibler, *Polym. Chem.* **2015**, 6, 4271.
- [34] B. T. Michal, C. A. Jaye, E. J. Spencer, S. J. Rowan, *ACS Macro Lett.* **2013**, 2, 694.
- [35] B. T. Michal, E. J. Spencer, S. J. Rowan, *ACS Appl. Mater. Interfaces* **2016**, 8, 11041.
- [36] G. L. Grocke, H. Zhang, S. S. Kopfinger, S. N. Patel, S. J. Rowan, *ACS Macro Lett.* **2021**, 10, 1637.
- [37] J. M. A. Carnall, C. A. Waudby, A. M. Belenguer, M. C. A. Stuart, J. J.-P. Peyralans, S. Otto, *Science* **2010**, 327, 1502.
- [38] U. F. Fritze, M. Von Delius, *Chem. Commun.* **2016**, 52, 6363.
- [39] Z. Q. Lei, H. P. Xiang, Y. J. Yuan, M. Z. Rong, M. Q. Zhang, *Chem. Mater.* **2014**, 26, 2038.
- [40] M. Pepels, I. Filot, B. Klumperman, H. Goossens, *Polym. Chem.* **2013**, 4, 4955.
- [41] Y. Li, Y. Zhang, O. Rios, J. K. Keum, M. R. Kessler, *RSC Adv.* **2017**, 7, 37248.
- [42] Z. Wang, Q. He, Y. Wang, S. Cai, *Soft Matter* **2019**, 15, 2811.
- [43] Q. He, Z. Wang, Y. Wang, Z. Song, S. Cai, *ACS Appl. Mater. Interfaces* **2020**, 12, 35464.
- [44] S. Huang, Y. Shen, H. K. Bisoyi, Y. Tao, Z. Liu, M. Wang, H. Yang, Q. Li, *J. Am. Chem. Soc.* **2021**, 143, 12543.
- [45] B. D. Fairbanks, T. F. Scott, C. J. Kloxin, K. S. Anseth, C. N. Bowman, *Macromolecules* **2009**, 42, 211.
- [46] A. B. Lowe, C. E. Hoyle, C. N. Bowman, *J. Mater. Chem.* **2010**, 20, 4745.
- [47] C. E. Hoyle, C. N. Bowman, *Angew. Chem. Int. Ed.* **2010**, 49, 1540.
- [48] S. V. Arehart, C. Pugh, *J. Am. Chem. Soc.* **1997**, 119, 3027.
- [49] Y.-K. Lee, K. Onimura, H. Tsutsumi, T. Oishi, *Polym. J.* **2000**, 32, 395.
- [50] M. Barnes, S. Cetinkaya, A. Ajnsztajn, R. Verduzco, *Soft Matter* **2022**, 18, 5074.
- [51] H. Kim, J. M. Boothby, S. Ramachandran, C. D. Lee, T. H. Ware, *Macromolecules* **2017**, 50, 4267.
- [52] M. O. Saed, R. H. Volpe, N. A. Traugutt, R. Visvanathan, N. A. Clark, C. M. Yakacki, *Soft Matter* **2017**, 13, 7537.
- [53] W. H. Carothers, *Trans. Faraday Soc.* **1936**, 32, 39.
- [54] N. J. Bongiardina, S. M. Soars, M. Podgorski, C. N. Bowman, *Polym. Chem.* **2022**, 13, 3991.
- [55] S. M. Soars, N. J. Bongiardina, B. D. Fairbanks, M. Podgorski, C. N. Bowman, *Macromolecules* **2022**, 55, 55.
- [56] J. T. Kamps, S. M. Soars, N. J. Bongiardina, B. D. Fairbanks, C. N. Bowman, *Tetrahedron* **2022**, 109, 10.
- [57] M. O. Saed, A. H. Torbati, C. A. Starr, R. Visvanathan, N. A. Clark, C. M. Yakacki, *J. Polym. Sci. B: Polym. Phys.* **2017**, 55, 157.
- [58] M. T. Sims, L. C. Abbott, R. M. Richardson, J. W. Goodby, J. N. Moore, *Liq. Cryst.* **2019**, 46, 11.
- [59] J. J. Hermans, P. H. Hermans, D. Vermaas, A. Weidinger, *Recl. Des Trav. Chim. Des Pays Bas* **1946**, 65, 427.
- [60] L. Zhang, L. Chen, S. J. Rowan, *Macromol. Chem. Phys.* **2017**, 218, 1.
- [61] B. R. Elling, W. R. Dichtel, *ACS Cent. Sci.* **2020**, 6, 1488.
- [62] S. Patai, Z. Rappoport, *Sulphur-Containing Functional Groups (1993)*, John Wiley & Sons, Inc., Chichester, UK **1993**.
- [63] J. J. Lessard, K. A. Stewart, B. S. Sumerlin, *Macromolecules* **2022**, 55, 10052.

## SUPPORTING INFORMATION

Additional supporting information can be found online in the Supporting Information section at the end of this article.

**How to cite this article:** C. A. Lindberg, E. Ghimire, C. Chen, S. Lee, N. D. Dolinski, J. M. Dennis, S. Wang, J. J. de Pablo, S. J. Rowan, *J. Polym. Sci.* **2023**, 1. <https://doi.org/10.1002/pol.20230547>